Optical 2-D Fourier Transform Spectroscopy of Excitons in Semiconductor Nanostructures

Steven T. Cundiff, *Senior Member, IEEE*, Alan D. Bristow, Mark Siemens, Hebin Li, Galan Moody, Denis Karaiskaj, Xingcan Dai, and Tianhao Zhang

(Invited Paper)

***Abstract*—Optical 2-D Fourier transform spectroscopy is a powerful technique for studying resonant light-matter interactions, determining the transition structure and monitoring dynamics of optically created excitations. The ability to separate homogeneous and inhomogeneous broadening is one important capability. In this paper, we discuss the use of this technique to study excitonic transitions in semiconductor nanostructures. In quantum wells, the effects of structural disorder is observed as inhomogeneous broadening of the exciton resonances. In quantum dots, the temperature dependence of the homogeneous width gives insight into the nature of the dephasing processes.**

***Index Terms*—Semiconductor nanostructures, spectroscopy, ultrafast optics.**

I. Introduction

COHERENT light-matter interactions in direct-gap semiconductor heterostructures are an important area of study in quantum electronics [1]. Understanding of these interactions provides a test for the theory of many-body systems and can help facilitate the design of optoelectronic devices. Nonlinear spectroscopic techniques, such at transient four-wave-mixing (TFWM), are the traditional approach to accessing the coherent response. However, recent developments in implementing multidimensional Fourier transform techniques in the optical regime have provided a new tool for these studies.

Multidimensional Fourier-transform spectroscopy was originally developed in nuclear magnetic resonance [2]. Over the last 10 years, there has been significant effort to implement it in the infrared and visible parts of the spectrum [3], [4]. Much of this work has focused on electronic and vibrational transitions in molecules and only considers two frequency (or time) variables, thus is known as 2-D Fourier transform (2-DFT) spectroscopy.

2-DFT spectroscopy has proven to be a powerful tool for unraveling the complex coherent response of exciton resonances in semiconductors. Early results gave evidence for coupling between excitonic resonances and to unbound electron–hole pairs [5]. Phase resolving the signal gave evidence for the dominance of many-body interactions [6]. The presence of contributions from correlation terms beyond a mean-field theory was verified in detailed comparison to microscopic calculations [7]. Using colinearly polarized excitation reveals contributions from biexcitonic resonances, which are more apparent for cross-linearly polarized excitation due to suppression of the many-body contributions [8]. By changing the excitation sequence, two-quantum transitions can be isolated [9], [10], which reveal pathways that occur at the mean-field level, due to the greater sensitivity to interactions.

In this paper, we present recent work using 2-DFT spectroscopy to study semiconductor nanostructures, where the exciton resonances display inhomogeneous broadening due to structural fluctuations. We review the experimental technique and the theoretical basis for extracting quantitative information about the linewidths from the 2-DFT spectrum of a resonance where the broadening is due to a mixture of homogeneous and inhomogeneous effects. In high quality quantum wells, inevitable monolayer fluctuations in the well width results in fluctuations of the confinement energy, which in turn gives rise to inhomogeneous broadening. However, the observed inhomogeneity reflects the interplay between the spatial frequencies of the monolayer fluctuations and the exciton Bohr radius, which is revealed as a difference in the inhomogeneous broadening of the heavy- and light-hole excitons, although they experience the same structure. Well-width fluctuations can be exploited to realize quantum dot states by decreasing the well width, thus increasing the fractional effect of a monolayer change in the width. In this case, fluctuations in the lateral size of the quantum dots results in strong inhomogeneous broadening. 2-DFT spectra reveal that within the inhomogeneous distribution, the scattering by phonons varies.

Manuscript received December 13, 2010; revised February 10, 2011; accepted February 15, 2011.

S. T. Cundiff and G. Moody are with JILA, University of Colorado and National Institute of Standards and Technology, Boulder, CO 80309 USA and also with the Department of Physics, University of Colorado, Boulder, CO 80309 USA (e-mail: cundiff@jila.colorado.edu; galan.moody@colorado.edu).

A. D. Bristow was with JILA, University of Colorado and National Institute of Standards and Technology, Boulder, CO 80309 USA. He is now with the Department of Physics, West Virginia University, Morgantown, WV 26506 USA (e-mail: alan.bristow@mail.wvu.edu).

M. Siemens was with JILA, University of Colorado and National Institute of Standards and Technology, Boulder, CO 80309-0440 USA. He is now with the Department of Physics and Astronomy, University of Denver, Denver, CO 80208-0183 USA (e-mail: msiemens@du.edu).

H. Li is with JILA, University of Colorado and National Institute of Standards and Technology, Boulder, CO 80309 USA (e-mail: hebin.li@jila.colorado.edu).

D. Karaiskaj was with JILA, University of Colorado and National Institute of Standards and Technology, Boulder, CO 80309 USA. He is now with the Department of Physics, University of South Florida, Tampa, FL 33620 USA (e-mail: karaiskaj@usf.edu).

X. Dai was with JILA, University of Colorado and National Institute of Standards and Technology, Boulder, CO 80309 USA. He is now with the Department of Physics, Tsinghua University, Beijing 1000084, China (e-mail: XingcanDai@mail.tsinghua.edu.cn).

T. Zhang was with JILA, University of Colorado and National Institute of Standards and Technology, Boulder, CO 80309 USA. He is now with the College of Nanoscale Science and Engineering, State University of New York at Albany, Albany, NY 12203 USA (e-mail: TZhang@uamail.albany.edu).

Color versions of one or more of the figures in this paper are available online at http://ieeexplore.ieee.org.

Digital Object Identifier 10.1109/JSTQE.2011.2123876

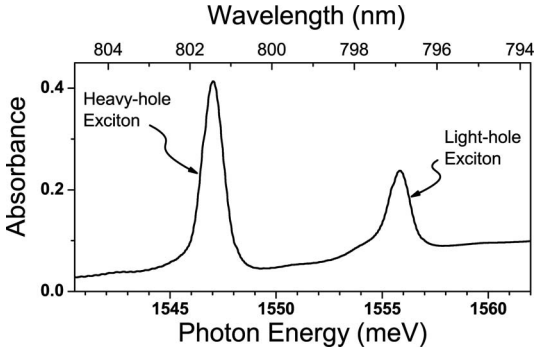

Fig. 1. Low temperature linear absorption spectrum of a quantum well where the degeneracy between heavy-hole and light-hole bands is lifted by quantum confinement, resulting in two exciton resonances.

A. Semiconductor Excitons

Absorption of light in a semiconductor produces an electron-hole pair by exciting an electron from the valence band to the conduction band. In GaAs, which is a direct-gap semiconductor, the maximum of the valence band and the minimum of the conduction band are aligned in momentum space. Direct-gap semiconductors are good light emitters because the electron and hole can recombine and conserve momentum. In addition, excitons can form in direct-gap semiconductors. An exciton is an electron-hole pair that is bound by the Coulomb attraction. In a perfect crystal, the center-of-mass wave function is extended, just as wave functions for the electronic states are. However, the binding results in a hydrogenic wave function for the relative coordinate between the electron and hole. The small masses of the electron and hole as well as the large background dielectric constant result in a binding energy of only a few millielectron-volts (meV). Consequently, excitons in GaAs only exist at low temperatures (tens of degrees Kelvin). The correlation between the electron and hole in an exciton increases their overlap, and hence their dipole moment. As a consequence, excitonic resonances tend to dominate the low temperature optical spectra of GaAs and GaAs nanostructures.

Fig. 1 shows the linear absorption spectrum of a typical GaAs quantum-well sample at low temperature. This sample consists of four layers of GaAs, each 10 nm thick, embedded between layers of $Al_{0.3}Ga_{0.7}As$, also 10 nm thick. Since $Al_{0.3}Ga_{0.7}As$ has a larger band gap than GaAs, carriers in the GaAs layer experience quantum confinement in the growth direction. The two resonances visible in the absorption spectrum are due to transitions from the heavy-hole (HH) and light-hole (LH) valence bands to the conduction band resulting in the formation of bound excitons. In bulk GaAs, the HH and LH bands are degenerate at $k = 0$, however, quantum confinement lifts the degeneracy because the confinement energy depends on mass.

B. Coherent Spectroscopy of Excitons

The original goal of studying excitons in semiconductors using coherent spectroscopy was to measure the dephasing rate despite the presence of inhomogeneous broadening. However, the measured signals had unexpected features, which were explained by the presence of many-body effects. Indeed it became clear that the coherent response is dominated by many-body effects. Thus, the study of many-body effects became an important goal in of itself.

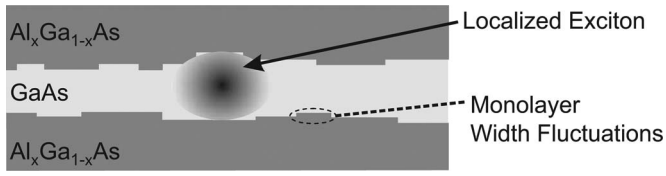

Fig. 2. Schematic showing disorder in a GaAs quantum well due to monolayer fluctuations of the well width.

Most of these studies used TFWM with two excitation pulses. The two pulses excite the sample with wave vectors $\mathbf{k}_a$ and $\mathbf{k}_b$. They are separated by a delay τ, where by definition $\tau > 0$ if the pulse with wave vector $\mathbf{k}_a$ arrives first. A signal is generated in the direction $\mathbf{k}_s = 2\mathbf{k}_b - \mathbf{k}_a$ by the coherent interaction between the incident pulses. If the sample consists of an ensemble of two-level systems, a signal is emitted in this direction only if $\mathbf{k}_a$ arrives before $\mathbf{k}_b$ [11]. The generation of the coherent TFWM signal is usually described using the following steps: 1) the first pulse creates a coherence in the sample; 2) the second pulse generates an excited-state or ground-state population from the coherence left behind by the first pulse, depending on the phase between the pulses, which varies across the sample; and c) the second pulse also scatters off the spatially modulated populations, which effectively act as diffraction gratings. If a slow, time-integrating, detector is used to detect the signal, the signal strength for a homogeneously broadened system will be $I_h(\tau) = e^{-2\gamma_{\rm ph}\tau}$, where $\gamma_{\rm ph}$ is the dephasing rate.

Measurements on semiconductor excitons did not agree with this simple picture in that there was a signal for $\tau < 0$. This discrepancy is due to the presence of many-body interactions is semiconductors, which dominate the coherent response. In a phenomenological picture, these signals can be assigned to local fields [12], [13], excitation induced dephasing [14]–[16], biexcitonic effects [17] and excitation-induced shifts [18], [19]. In a microscopic calculation, they appear from a combination of mean-field effects and correlation terms beyond a mean field [20]–[22].

Quantum wells exhibit inhomogeneous broadening of the resonance due to structural disorder, namely fluctuations in the well width by one monolayer (see Fig. 2). In the presence of inhomogeneous broadening, TFWM produces a photon echo. In this case, the time-integrated signal intensity is $I_h(\tau) = e^{-4\gamma_{\rm ph}\tau}$. Thus, TFWM can still measure the dephasing rate even when the resonance is inhomogeneously broadened, however, the relationship between the decay of the signal and dephasing rate is different by a factor of two. This means that knowledge about the nature of the broadening is needed before a dephasing rate can be extracted from the TFWM decay. In addition to inhomogeneous broadening of the resonance, structural disorder localizes the exciton center-of-mass wave function, which can reduce or suppress many-body interactions and simplify the interpretation of the data.

II. METHOD

Multidimensional Fourier transform spectroscopy utilizes a signal that is produced by the nonlinear mixing of incident electromagnetic fields in a sample. Typically pulsed excitation fields are used and the signal is recorded in the time domain as a function of the delays between the excitation pulses. To produce a spectrum, a multidimensional Fourier transform is taken numerically with respect to the delays and signal time. In order to take the Fourier transform, the data must be recorded with equal time steps that have subwavelength precision and stability.

The first proposal to implement multidimensional Fourier transform spectroscopy using a Raman excitation scheme was made in 1993 [23]. The proposal focused on studying vibrational excitations in molecules, which proved easier to do using direct infrared excitation [24], [25]. 2-DFT spectroscopy has also been implemented using visible or near-IR pulses to study electronic excitations in dye molecules [26] and in photosynthetic systems [27].

2-DFTS is typically implemented using three excitation pulses with wave vectors $\mathbf{k}_a$, $\mathbf{k}_b$, and $\mathbf{k}_c$. These pulses interact in the sample to produce a signal in the direction $\mathbf{k}_s = -\mathbf{k}_a + \mathbf{k}_b + \mathbf{k}_c$. Pulses $\mathbf{k}_a$ and $\mathbf{k}_b$ are separated by a delay τ, while pulses $\mathbf{k}_b$ and $\mathbf{k}_c$ are separated by delay T. The signal is recorded as a function of time t. The resulting three dimensional time domain "spectrum" is denoted $S_i(\tau, T, t)$, where the subscript i denotes the time ordering of the conjugated field $\mathbf{k}_a$. If $\mathbf{k}_a$ arrives first, the resulting $S_I(\tau, T, t)$ separates inhomogeneous and homogeneous broadening because the phase accumulated during τ is cancelled during t, which also produces a photon echo in a TFWM experiment. This cancelation does not occur if $\mathbf{k}_a$ arrives second to produce an $S_{II}(\tau, T, t)$, however, the sum of $S_I(\tau, T, t)$ and $S_{II}(\tau, T, t)$ produces a "correlation" spectrum that isolates the absorptive part of the nonlinear response [28]. 2-D frequency domain spectra are obtained by Fourier transforming two of the time variables while holding the third fixed. The most common 2-D spectrum is $S_I(\omega_\tau, T, \omega_t)$ as it reveals the homogeneous linewdith.

A. Overview of 2-DFT Spectroscopy of Semiconductors

The power of measuring the TFWM signal from semiconductor excitons as a function of multiple delays (or frequencies) was first recognized in the context of understanding the origin of beats in the time-integrated TFWM signal. The origin of beats arising from simultaneous excitation of HH and LH resonances was clear [29]. However, those arising from monolayer fluctuations were more controversial [30]. Specifically, debate arose as to whether the observed beats were truly due to quantum mechanical interference, and thus "quantum beats" or rather were only due to electromagnetic interference, which was known as "polarization interference." It was shown that measuring the time-resolved TFWM signal for a series of delays [31], or measuring the signal spectrum for a series of delays [32] could distinguish between these cases. Applying these methods to the case of monolayer fluctuations showed a complex situation due to the interplay between disorder and many-body effects [33], [34].

A variant on these techniques, known as "coherent excitation spectroscopy" generated a 2-D frequency spectrum by resolving the TFWM signal produced by a narrow band first pulse and a broadband second pulse, and plotting the spectra for varying first pulse frequencies [35]. This approach was motivated by earlier work using such a pulse combination to study coupling between the excitons and continuum states and amongst magnetoexcitons [36].

While these experiments were addressing similar questions to those answered by 2-DFTS, namely, whether or not resonances are homogeneously or inhomogeneously broadened and whether or not multiple resonances are coupled, they had significant limitations compared to 2-DFTS experiments. Since they did not measure the complex signal field, they could not separate real and imaginary parts. Furthermore, most of these experiments only used two excitation pulses, thus, many contributing quantum pathways could not be separated.

The first demonstration of 2-DFT spectroscopy of exciton resonances in a semiconductor quantum well measured the amplitude spectrum of the HH and LH excitonic resonances [5]. These spectra showed that an HH-LH cross-peak was the strongest feature and that the continuum produced a streak parallel to the ω_τ axis, rather than the diagonal streak expected for an inhomogeneously broadened system. Simulations using modified optical Bloch equations reproduced these features, but only when phenomenological many-body interactions were included. Determining the overall phase, so that the real and imaginary spectra could be generated [6], gave further insight into the many-body interactions and showed that excitation-induced shifts [19] dominate.

Calculations using a microscopic theory confirmed that 2-DFT spectra clearly show signatures of many-body interactions [37]. Detailed comparison to experiments showed correlation terms beyond a mean-field approach are required to obtain agreement with the experiments [7]. A study of the polarization dependence showed biexcitonic contributions for colinearly polarized excitation pulses, but the biexcitonic contributions become more important for cross-linearly polarized excitation pulses, because the many-body enhancement of the exciton peak is absent [8], [38].

One of the powerful features of 2-DFT spectroscopy is its ability to probe nonradiative coherences, i.e., coherences between states that are not coupled by a dipole allowed transition [39]. In semiconductors, examples of non-radiative coherences include the "Raman" coherence between the HH and LH exciton [40] and two-quantum coherences between the ground state and two-exciton states, which include bound biexcitons and unbound two-exciton pairs [9], [10], [38], [41]. Theory shows that two-exciton two-quantum coherences appear within a mean field approximation [10], which is an interesting contrast to the single-quantum coherences that required correlation terms beyond mean-field to yield agreement with experiment [7].

The ability of 2-DFT spectroscopy to separate the inhomogeneous and homogeneous components of the line broadening, and moreover to measure the homogeneous linewidth in the presence

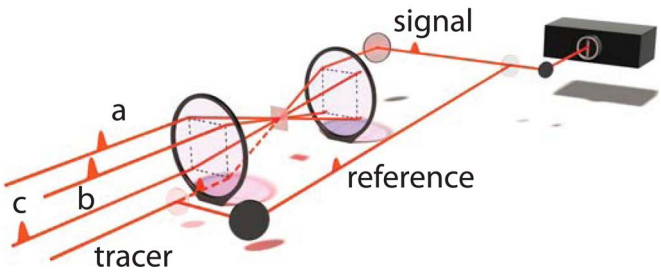

Fig. 3. Diagram of experimental arrangement for excitation and detection of the sample.

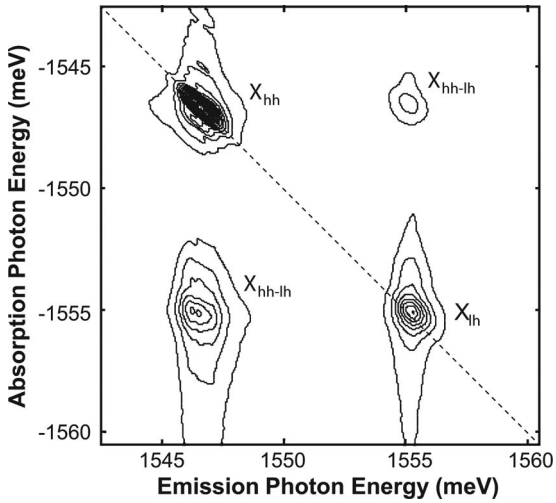

Fig. 4. Rephasing spectrum $S_I(\omega_\tau, T, \omega_t)$ of a GaAs quantum well excited with cocircular excitation pulses. The dashed line indicates the diagonal.

of inhomogeneous broadening, is significant in semiconductors due to structural disorder in quantum wells and size dispersion in quantum dots. Two methods have been proposed to quantify the homogeneous width, 1) using the cross-diagonal distance between the maximum and minimum in a phase-rotated real spectrum [42]; and 2) fitting the cross-diagonal line shape in the amplitude spectrum [43]. These techniques are discussed below. They have been used to study disordered quantum wells [44] and broadening of natural quantum dots that occur due to interface fluctuations in thin quantum wells [45]. Single semiconductor quantum dots have also been studied using an alternate approach to 2-DFT based on heterodyne spectral interferometry [46], [47].

B. Experimental Implementation

The excitation pulses are produced by a set of nested interferometers to produce four phase-locked beams that propagate parallel to each other on four corners of a square [48]. The input to the interferometers is the output of a modelocked laser that produces 100 fs pulses at a repetition rate of 76 MHz. The interferometers are locked using a copropagating helium–neon (He–Ne) laser beam. The individual servo locks can be disabled under computer control, allowing the arm lengths to be changed while the computer monitors the He–Ne interference fringes. After the length has been changed by a desired number of fringes, the servo loop is reenabled. Thus, the delays between the pulses are controlled and stabilized with interferometric precision.

Three of the beams generated by the interferometers are focused on to the sample by a lens (Fig. 3). The interaction of the three beams produces a signal beam corresponding to the fourth corner of the square. The fourth incident beam is split in two parts. One part is routed around the sample and recombined with the signal as the reference beam for retrieving the complex signal spectrum using spectral interferometry [49]. This beam is phase-locked to excitation pulse c. The second part is used to determine phase shifts along the signal path and is blocked when spectra are being acquired.

The real and imaginary parts of the 2-DFT spectrum are related to the complex third-order susceptibility. To properly decompose the spectrum into real and imaginary parts, corrections must be made for phase offsets in the as-measured spectrum. To determine these offsets, we image the interference pattern of the four incident beams and measure the phase of the reference pulse relative to the tracer beam [50]. A similar method has been used for infrared 2-DFT experiments [51].

C. $S_I(\omega_\tau, T, \omega_t)$ of Excitons in Quantum Wells

A typical rephasing spectrum $S_I(\omega_\tau, T, \omega_t)$ for a GaAs quantum well is shown in Fig. 4. This spectrum is for an epitaxially grown sample containing a four-period multiple QW with $Al_{0.3}Ga_{0.7}As$ barriers. Both the wells and barriers are 10 nm thick. The sample is mounted on a sapphire disk and GaAs substrate is removed for transmission experiments. The sample is held at 6 K in a cold-finger cryostat. The linear absorption spectrum of this sample is presented in Fig. 1. The HH and LH exciton peaks are separated by 8 meV, and both are excited by the laser, which has a spectral width of approximately 11 meV full-width half-maximum. For this spectrum, the polarizations of the excitation beam are cocircular and the same polarization signal is detected.

When plotting 2-DFT spectra, we use the convention that the signal field defines the sign of the frequency. Since the first pulse is conjugated in an S_I spectrum, the absorption frequency, ω_τ, is negative because it has the opposite sign from the emission frequency, ω_t. Thus, the absorption frequency axis is inverted in an S_I spectrum. To help indicate this, we plot the diagonal, $\omega_t = -\omega_\tau$ as a dashed line.

As mentioned above, the important characteristics of the 2-DFT spectra in Fig. 4 are diagonal intra-action resonances of the two exciton species, two off-diagonal interaction resonances, and vertical stripes associated with excitation of *e–hh* continuum states. In phase-resolved real 2-DFT spectra (not shown here) the line shapes of most features are dispersive, resulting from many-body interactions, particularly excitation-induced shifts [6] in a phenomenological description. Qualitatively, these spectra match well to microscopic 1-D tight-binding calculations, which include Coulomb correlations beyond the Hartree-Fock mean-field approximation [7] and phenomenological Gaussian inhomogeneous broadening [42]. More recently,

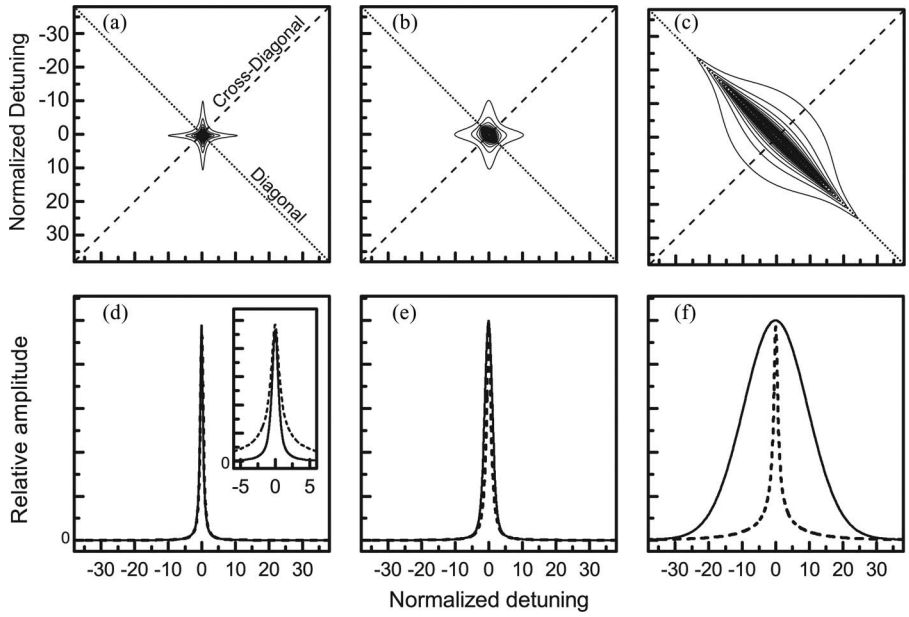

Fig. 5. Rephasing 2-DFT spectra and slices for varying ratios of homogeneous and inhomogeneous broadening. (a)–(c) 2-DFT spectra, (d)–(f) diagonal (solid line) and cross-diagonal (dashed line) slices of the 2-DFT spectra. For (a) and (d), there is no inhomogeneous broadening, for (b) and (e) the inhomogeneous broadening matches the homogeneous broadening, and in (c) and (f) the inhomogeneous broadening is much larger than the homogeneous broadening. The frequency scales are normalized to the homogeneous width. The inset in (d) compares the cross diagonal slices for homogeneous broadening (solid line) and inhomogeneous broadening (dashed line).

the inhomogeneous broadening has been modeled with multiple realizations of fluctuating energy levels to simulate structural disorder—a more realistic microscopic picture—and has again shown good qualitative agreement with experimental spectra [52].

III. Line Shape Analysis

Multidimensional NMR spectroscopy focuses on peak strengths to extract coupling information and largely ignores information in the 2-D line shape, beyond correcting phase twists and determining peak amplitudes [2]. In 2-D infrared spectroscopy, homogeneous and inhomogeneous line shapes have been considered in molecules [53]. The linewidths of inhomogeneously broadened resonances in the diagonal and cross-diagonal directions of a rephasing $S_I(\omega_\tau,T,\omega_t)$ 2-DFT spectrum are significantly different. Inhomogeneous broadening results in elongation along the diagonal of a $S_I(\omega_\tau,T,\omega_t)$ spectrum. It is, therefore, possible to extract both the homogeneous linewidth (γ) and inhomogeneous linewidth ($\delta\omega$) from a single $S_I(\omega_\tau,T,\omega_t)$ spectrum. Diagonal and cross-diagonal slices in the $S_I(\omega_\tau,T,\omega_t)$ spectra can be analyzed [54] by applying the projection-slice theorem [2] to the 2-D time data. The projection-slice theorem relates a projection in one domain to a slice in the Fourier-transformed domain (even in multiple dimensions). Tokmakoff used this method to extract γ and $\delta\omega$ for two extreme cases [54]: 1) for a purely homogeneous line shape ($\delta\omega = 0$), and 2) for a strongly inhomogeneous line shape ($\delta\omega \gg \gamma$).

For excitonic resonances in semiconductors, the weak inhomogeneous regime ($\delta\omega \simeq \gamma$) is also of importance. Recently, methods have been proposed to relate theoretical values of γ and $\delta\omega$ to the line shapes found in experiments. In one method, the peak-to-peak distances along the dispersive directions of phase-resolved $S_I(\omega_\tau,T,\omega_t)$ and $S_{II}(\omega_\tau,T,\omega_t)$ spectra are extracted [42]. The peak-to-peak distance from the $S_I(\omega_\tau,T,\omega_t)$ spectrum, $\Delta\Omega_{\mathrm{R}}$, is proportional to γ. The value from the $S_{II}(\omega_\tau,T,\omega_t)$ spectrum, $\Delta\Omega_{\mathrm{NR}}$, contains contributions from inhomogeneous and homogeneous broadening, such that $\Delta\Omega_{\mathrm{NR}} - \Delta\Omega_{\mathrm{R}} = \Delta\Omega_{\mathrm{NR-R}} \propto \delta\omega$. Model calculations show that $\Delta\Omega_{\mathrm{R}} \simeq 0.9 \times \gamma$, whereas $\Delta\Omega_{\mathrm{NR-R}}$ is approximately equal to the inhomogeneous width [55].

A second method of relating the observed line shape to γ and $\delta\omega$ extends the analysis developed by Tokmakoff. Starting with a perturbative solution of the optical Bloch equations for the TFWM signal in the time domain, analytical expressions for the calculated signal can be manipulated using the slice-projection theorem rather than performing the usual 2-DFT [43]. The diagonal of the 2-D time map is dominated by dephasing for both homogeneously and inhomogeneously broadened spectra. Projection of the time data onto the diagonal yields a 1-D function that will mostly represent the homogeneous dephasing, but will be modified by the inhomogeneous broadening. Similarly, a projection of the time data onto a line through the origin and perpendicular to the diagonal gives a function that is dominated by inhomogeneous broadening. Fourier-transforming these projections yields slices in the 2-DFT spectra that correspond to the diagonal ($\omega_{\tau'}$) and cross-diagonal ($\omega_{t'}$) directions (see Fig. 5), with an appropriate frequency offset. The functional forms of these slices can be used to fit the diagonal and cross-diagonal slices of a rephasing 2-DFT spectrum.

In the limit of weak inhomogeneous broadening, γ and $\delta\omega$ contribute to both the diagonal and cross-diagonal slices of the 2-DFT line shape. The functional forms for line shape slices

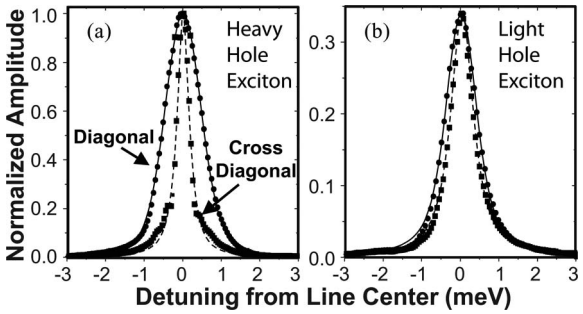

Fig. 6. Diagonal (circles) and cross-diagonal (squares) slices of 2-DFT spectrum shown in Fig. 4 for the (a) heavy-hole and (b) light-hole exciton resonances. The solid (dashed) lines show the fits for the diagonal (cross-diagonal) lines.

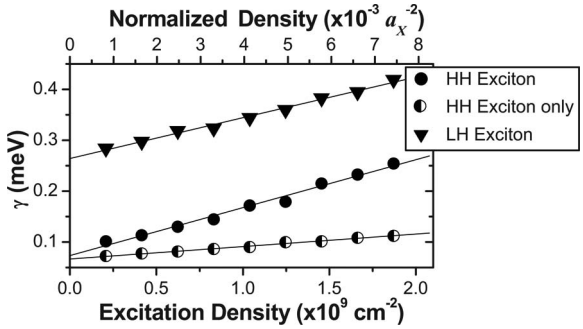

Fig. 7. Excitation-density dependence of the homogeneous line width extracted from the rephasing 2-DFT spectra for both exciton species and for the HH exciton when excited alone. Solid lines are linear fits for the excitation-induced homogeneous linewidth change.

with arbitrary inhomogeneity are

$$S(\omega_{\tau'}) = \frac{1}{\gamma\delta\omega\sqrt{2/\pi}}\exp\{x_-^2\} \times \left(\mathrm{Erfc}[x_-] + \exp\left\{\frac{2i\gamma\omega_{\tau'}}{\delta\omega^2}\right\}\mathrm{Erfc}[x_+]\right) \quad (1)$$

$$S(\omega_{t'}) = \frac{\exp\{x_-^2\}\mathrm{Erfc}\{x_-\}}{\delta\omega(\gamma - i\omega_{t'})} \quad (2)$$

where $\mathrm{Erfc}(x)$ is the complex complementary error function and $x_\pm = \frac{\gamma \pm i\omega_{\tau'}}{\sqrt{2}\delta\omega}$. Examples of 2-DFT spectra and diagonal and cross-diagonal slices for single resonances that are homogeneously broadened, have equal homogeneous and inhomogeneously broadening and that have strong inhomogeneous broadening are shown in Fig. 5. Complete details of this analysis is given in Siemens *et al.* [43].

IV. Disordered Quantum Wells

To extract information about the broadening mechanism for excitons in GaAs quantum wells [44], we apply the line shape analysis presented in the previous section to the 2-DFT spectrum shown in Fig. 4. Fig. 6 shows the diagonal and cross-diagonal data slices and fits using (1) and (2). The two slices can be fit simultaneously to obtain consistent values. Additionally, this analysis can be extended to find functional forms for slices in the nonrephasing spectrum. However, these fits are not as robust and do not provide any additional information, since the nonrephasing is formally equivalent to a 1-D scan. Including phenomenological many-body terms in the optical Bloch equations does not result in a significant change in the extracted linewidths.

A striking feature in the 2-DFT spectrum is the difference between diagonal and cross-diagonal widths for the HH exciton as compared to the LH exciton. For the HH exciton, the diagonal width is clearly larger than the cross-diagonal. Whereas, for the LH exciton, they are similar. In part, this difference is because the LH exciton has a larger homogeneous width than the HH exciton due to spectral overlap and coupling between the LH excitons with HH continuum states, which have a faster dephasing rate [56]. Also, the LH exciton actually has a smaller inhomogeneous width than the HH exciton. This difference means that while the HH exciton is dominated by disorder, the LH exciton is not.

The difference in the HH exciton and LH exciton inhomogeneous widths is initially surprising, but recent calculations explained this difference in terms of the Bohr radii (a_X) of the excitons and the length scale of the disorder potential (l_d) in the QW [52]. When $a_X \gg l_d$, the exciton averages over the disorder, whereas if $a_X \ll l_d$ there are no fluctuations for the exciton to sense. Between these extremes, when l_d is close to a_X and the excitonic localization length, the exciton is the most sensitive to the disorder [57]. The 2-D exciton Bohr radius is $a_X = \hbar^2\varepsilon_0/2\mu e^2$, thus the difference in a_X between the two excitons species is due the reduced excitonic mass, which is $\mu = m_e^* m_v^*/m_e^* + m_v^*$. The effective mass of the electron (m_e^*) is the same for both excitons, but the effective masses of the valence bands (m_v^*) differ, resulting in a_X of the LH exciton being approximately 50% larger than the HH exciton $a_X \sim 6$ nm. Thus we conclude that, for this sample, the magnitude of the disorder is larger for length scales close to the HH Bohr radius than for length scales comparable to the LH Bohr radius.

Disorder-induced and other broadening mechanisms are clearly separated by 2-DFT spectroscopy. The excitation-induced dephasing contribution to the coherent response can be determined from the variation of the homogeneous line width in excitation-density-dependent measurements, performed in the $\chi^{(3)}$ regime [14], [16], [58]. Fig. 7 shows the extracted 1) homogeneous and 2) inhomogeneous linewidths as a function of excitation power of the HH exciton and LH exciton when the laser has sufficient bandwidth to excite both resonances simultaneously. From these data, the linewidth at zero excitation density can be determined by extrapolation. Also shown are the linewidths for the HH exciton when excited alone by spectrally filtered laser pulses.

Over the range of excitation densities shown in Fig. 7, the homogeneous linewidth increases by approximately 0.15 meV for HH and LH excitons, i.e., the two slopes are $\sim 9 \times 10^{-11}$ meV/cm^{-2}, as determined by a linear fit. Although the excitons have different energies and oscillator strengths, they both experience similar amounts of excitation-induced dephasing. However, the zero-excitation homogeneous linewidths differ; extrapolated values are $\gamma_{0,HH} = 0.073 \pm 0.005$ meV and

$\gamma_{0,LH} = 0.26 \pm 0.003$ meV, which confirms that the LH exciton has a larger natural homogeneous linewidth.

Experiments performed with spectrally filtered excitation pulses excite only the HH excitonic resonance, suppressing excitation of the *e–hh* continuum or LH excitons. In this case, the slope of the homogeneous linewidth for the HH exciton decreases to $\sim 2 \times 10^{-11}$ meV/cm^{-2}. However, the extrapolated natural homogeneous linewidth is unchanged within experimental errors. This difference in slopes demonstrates that exciton-exciton scattering, and exciton-free-carrier scattering mechanisms significantly contribute to the excitation-induced dephasing of the HH excitonic resonance [56].

V. Natural Quantum Dots

If the quantum wells are made very thin, and the growth is optimized for formation of large islands, the disorder mentioned in the previous section can result in well-localized states called "interface fluctuation quantum dots." These quantum dots (QDs) are a model zero-dimensional system for investigating coherent exciton and carrier interactions because of their discrete energy level structure [59]–[62], narrow homogeneous linewidth [63], large oscillator strength [64], and defect-free growth. The homogeneous linewidth of the exciton depends on the QD environment, such as lattice temperature T_L, exciton population density, and material composition.

Using 2-DFT spectroscopy, we measure the temperature dependence of the homogeneous linewidth at line center of an inhomogeneously broadened QD ensemble in the temperature range of 6 to 50 K [45], and show that the measured linewidths agree with those obtained by prior studies of single QDs [65]. The temperature dependence of the linewidth exhibits an activation-type behavior; however lack of a phonon-activation peak in the 2-D spectra and comparison to theoretical predictions suggest that elastic exciton-phonon coupling via a virtual activation process of the ground state exciton dominates the thermal broadening. Measurement of the virtual activation energy and exciton-phonon coupling strength as a function of QD size shows that excitons localized in smaller QDs dephase faster. The exciton-phonon coupling is weak enough that broad sidebands are not observed.

The sample is an epitaxially grown single GaAs QW 15 monolayers (ML) thick, corresponding to ≈4.2 nm, with 35 nm $Al_{0.3}Ga_{0.7}As$ barriers. Growth interruption wait times on the order of tens of seconds at the GaAs/$Al_{0.3}Ga_{0.7}As$ interface result in monolayer width fluctuations forming island-like features known as interfacial or "natural" QDs. The QD ensemble is inhomogeneously broadened because of QD size dispersion. Excitons delocalized in the QW are also inhomogeneously broadened due to averaging of the wave function over high-frequency fluctuations at the $Al_{0.3}Ga_{0.7}As$/GaAs interface. The 2-DFT $S_I(\omega_\tau, T, \omega_t)$ for this sample is shown in Fig. 8. The homogeneous linewidths are obtained by fitting cross-diagonal peaks as above.

Fig. 9 shows the homogeneous linewidth across the inhomogeneous distribution for T_L from 6 to 50 K, with line center marked by circles. The linewidth increases linearly with increasing energy (decreasing QD size) across the inhomogeneous distribution for all temperatures. Oscillations in the linewidths are due to truncation in the time domain due to the finite scan range of τ used in experiments. To reduce the effect of truncation, we apply an arctangent window function, thus the actual line shape is a convolution of a Lorentzian, from the exponential decay and Fourier transform of the window function. However, importance of the window function oscillates depending on how many cycles of the "carrier frequency" fit within it (actually the aliased carrier due to undersampling). If there is an integer number of cycles, it has the smallest influence, whereas if there is an integer number plus a half cycle, it is the strongest. Thus, the contribution of the window function oscillates with frequency, and hence, so does the extracted linewidth. Of course, the truncation effects are stronger for slow dephasing, and thus at lower temperature. From the magnitude of the oscillations, it is easy to estimate that at most the window function is increasing the linewidth by 10% for the lowest temperatures. At each temperature, a linear fit to the extracted values of the homogeneous linewidth, which further reduces the effect of the windowing, and the values used for the following analysis are taken from the fit.

The temperature dependence of the homogeneous linewidth at line center is shown in Fig. 10. Thermal broadening of the

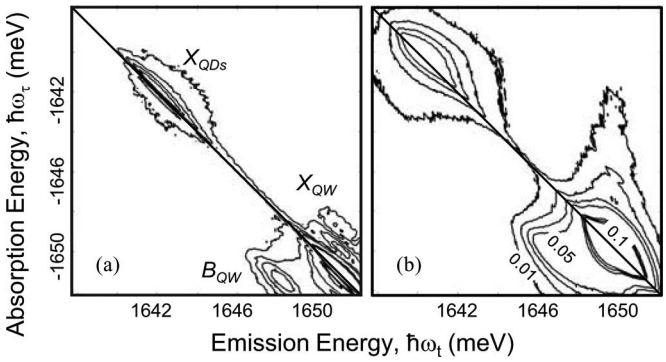

Fig. 8. Amplitude 2DFT spectrum (normalized to the QW peak and truncated to emphasize the QD signal) of QW and QD ensemble for $T_L = 6$ K (a) and 50 K (b). The QW and QD homogeneous linewidths increase and the spectral features redshift with temperature.

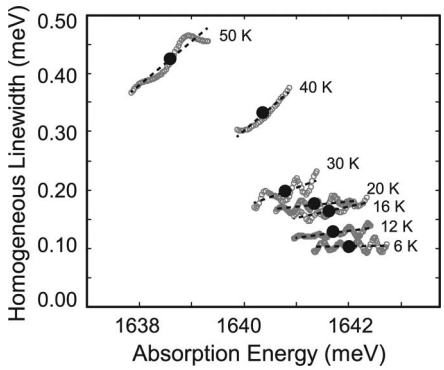

Fig. 9. The homogeneous linewidths across the inhomogeneous distribution for an average excitation photon density of 1×10^{12} photons/pulse/cm^2 are shown as a function of temperature. Line center is indicated by the solid circles.

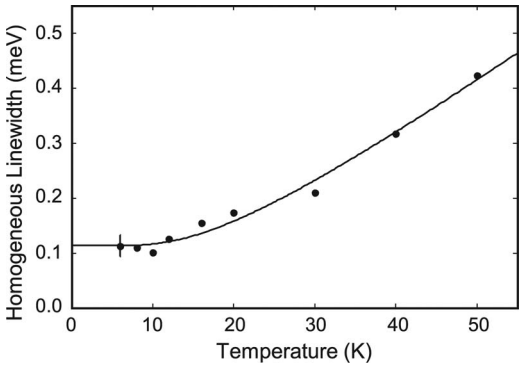

Fig. 10. Temperature dependence of the homogeneous linewidth for an average excitation power of 1.0 mW and T = 200 fs, with a representative error bar (high-low values) determined from repeating the measurement at $T_L = 6$ K. Equation (3) is fit to the data using an activation energy of $E_{12} = 4.44$ meV and an offset of $\gamma_1^* = 0.11$ meV. The absence of an activation peak in the 2-D spectra reveals that the dominant thermal broadening mechanism is *elastic* exciton-phonon scattering.

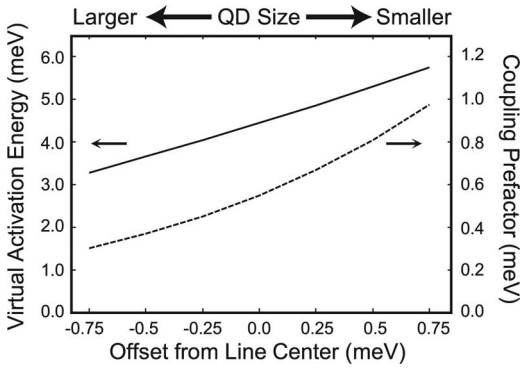

Fig. 11. Virtual activation energy (solid line) and exciton-phonon coupling prefactor (dashed line), obtained from fitting (3) to the homogeneous linewidth temperature dependence, increase across the inhomogeneous distribution.

linewidth for excitons in QDs has been modeled by considering the probability of phonon absorption and subsequent excitation of the exciton to higher-lying states [63]

$$\gamma_\mu(T) = \gamma_\mu^* + \sum_{\nu>\mu} \gamma_{\mu\nu} n(E_{\mu\nu}, T) \tag{3}$$

where $n(E_{\mu\nu}, T) = \left[e^{E_{\mu\nu}/k_b T} - 1\right]^{-1}$ is the Bose-Einstein distribution that gives the number of phonons at an energy $E_{\mu\nu}$. The first term in (3) is temperature-independent dephasing, while the second term is due to activation of the exciton from state μ to a higher-lying energy state ν.

We use a single term from the sum in (3) to fit the data, plotted as the solid line in Fig. 10, and extract an activation energy of $E_{12} = 4.44$ meV and an offset of $\gamma_1^* = 0.11$ meV. The offset is predominantly a result of excitation-induced dephasing. A solution to Schrödinger's equation as well as PLE spectra reveal discrete energy levels with a separation in the range of E_{12}. Activation to a real state would result in incoherent population being transferred from the initially excited state to the higher energy state. Such incoherent population dynamics are a form of spectral diffusion. For nonzero T, spectral diffusion results in off-diagonal peaks in 2-D spectra; in this case, they would appear above the diagonal by 4.44 meV as the population is transferred to a higher energy state. We have taken data for large T and do not observe such off diagonal peaks that would result from activation to a real state.

The lack of an activation peak indicates that the broadening is due to population decay and pure dephasing processes. Calculations in the approximation of linear coupling between excitons and acoustic phonons predict broad acoustic phonon sidebands on a narrow temperature-independent zero-phonon line, which has also been reproduced theoretically [66]. Including quadratic exciton-phonon coupling results in a temperature dependence of the zero-phonon line and predicts that the dephasing depends strongly on QD size and phonon energies [67]. This model yields a linear dependence of the dephasing rate on temperature if the energy separation between the QD ground and excited states is larger than the acoustic phonon energy because only virtual excitation of the QD lowest state contributes. When the temperature is increased so that the phonon energy approaches the QD level separation, a nonlinear temperature dependence appears due to participation of higher lying states in the virtual processes [67]. Sidebands on the zero-phonon line only appear for strong exciton-phonon coupling. Experimentally, both an exponential decay (corresponding to a Lorentzian zero-phonon line) [68] and sidebands [69] have been obtained for GaAs interface QDs. Sidebands have also been observed for InAs QDs [70]. The lack of sidebands can be attributed to smaller confinement in larger QDs [71].

In interfacial GaAs QDs with lateral dimensions of ≈40 nm, phonons with energies below 1 meV couple most strongly to excitons [67], [69]. Weak exciton confinement and ground-to-excited state energy level separation of a few meV result in a linear temperature dependence of the dephasing rate for $T_L <$ 20 K. At elevated temperatures, the thermal broadening is well-described by the same activation term that is used to fit the data in Fig. 10. Thus, the thermal broadening is dominated by virtual transitions of the ground state exciton via elastic exciton-phonon coupling, rather than inelastic phonon-assisted activation to higher-lying states.

The homogeneous linewidth temperature dependence as a function of energy offset from line center (QD size) was fit to (3). Fig. 11 shows the virtual activation energy, E_{12} (solid line), and the exciton-phonon coupling strength, γ_{12} (dashed line). Both increase with increasing exciton energy (decreasing QD size) across the inhomogeneous distribution. An increase in E_{12} results from the ground-to-excited state energy separation increasing with decreasing QD size. A solution to Schrödinger's equation shows that E_{12} changes by ± 0.99 meV for a change in exciton energy of ± 0.75 meV, which agrees well with the measured values of E_{12}.

A larger E_{12} for smaller QDs would indicate weaker thermal broadening; however, we observe an increase of the slope of the homogeneous linewidth with temperature (Fig. 9). Consequently, greater thermal broadening for smaller QDs is a result of larger exciton-phonon coupling, shown as the dashed line

in Fig. 11. The effect of γ_{12} dominates the effect of E_{12}, as predicted [67].

VI. Conclusion

We have shown that 2-DFT spectroscopy is a powerful technique for separating the homogeneous and inhomogeneous contributions to the broadening of spectral lines. Using this technique, we have studied the homogeneous linewidth of disordered quantum wells and natural quantum dots.

Acknowledgment

The authors thank R. P. Mirin, National Institute of Standards and Technology (NIST)-Boulder, for providing the quantum-well samples, D. Gammon and A. S. Bracker, National Research Laboratory (NRL), for providing the natural quantum dot sample and P. Thomas, T. Meier, and S. Mukamel for discussions. This work was funded by the the National Science Foundation, the U.S. Department of Energy, and the Chemical Sciences, Geosciences, and Biosciences Division Office of Basic Energy Sciences. M. E. Siemens acknowledges funding from the National Academy of Sciences/National Research Council postdoctoral fellows program.

References

[1] S. T. Cundiff, "Coherent spectroscopy of semiconductors," *Opt. Express*, vol. 16, pp. 4639–4664, 2008.

[2] R. R. Ernst, G. Bodenhausen, and A. Wokaun, *Principles of Nuclear Magnetic Resonance in One and Two Dimensions*. Oxford, U.K.: Oxford Science Publications, 1987.

[3] M. Cho, "Coherent two-dimensional optical spectroscopy," *Chem. Rev.*, vol. 108, pp. 1331–1418, 2008.

[4] D. Jonas, "Two-dimensional femtosecond spectroscopy," *Annu. Rev. Phys. Chem.*, vol. 54, pp. 425–463, 2003.

[5] C. N. Borca, T. H. Zhang, X. Q. Li, and S. T. Cundiff, "Optical two-dimensional Fourier transform spectroscopy of semiconductors," *Chem. Phys. Lett.*, vol. 416, pp. 311–315, 2005.

[6] X. Q. Li, T. H. Zhang, C. N. Borca, and S. T. Cundiff, "Many-body interactions in semiconductors probed by optical two-dimensional Fourier transform spectroscopy," *Phys. Rev. Lett.*, vol. 96, p. 057406, 2006.

[7] T. Zhang, I. Kuznetsova, T. Meier, X. Li, R. Mirin, P. Thomas, and S. Cundiff, "Polarization-dependent optical 2d fourier transform spectroscopy of semiconductors," *Proc. Nat. Acad. Sci.*, vol. 104, pp. 14 227–14 232, 2007.

[8] A. D. Bristow, D. Karaiskaj, X. Dai, R. P. Mirin, and S. T. Cundiff, "Polarization dependence of semiconductor exciton and biexciton contributions to phase-resolved optical two-dimensional fourier-transform spectra," *Phys. Rev. B*, vol. 79, p. 161305(R), 2009.

[9] K. W. Stone, K. Gundogdu, D. B. Turner, X. Li, S. T. Cundiff, and K. A. Nelson, "Two-quantum 2d ft electronic spectroscopy of biexcitons in gaas quantum wells," *Science*, vol. 324, pp. 1169–1173, 2009.

[10] D. Karaiskaj, A. D. Bristow, L. Yang, X. Dai, R. P. Mirin, S. Mukamel, and S. T. Cundiff, "Two-Quantum Many-Body Coherences in Two-Dimensional Fourier-Transform Spectra of Exciton Resonances in Semiconductor Quantum Wells," *Phys. Rev. Lett.*, vol. 104, no. 11, Mar. 2010.

[11] T. Yajima and Y. Taira, "Spatial optical parametric coupling of picosecond light-pulses and transverse relaxation effect in resonant media," *J. Phys. Soc. Japan*, vol. 47, pp. 1620–1626, 1979.

[12] K. Leo, M. Wegener, J. Shah, D. S. Chemla, E. O. Göbel, T. C. Damen, S. Schmitt-Rink, and W. Schäfer, "Effects of coherent polarization interactions on time-resolved degenerate 4-wave-mixing," *Phys. Rev. Lett.*, vol. 65, pp. 1340–1343, 1990.

[13] M. Wegener, D. S. Chemla, S. Schmitt-Rink, and W. Schäfer, "Line-shape of time-resolved 4-wave-mixing," *Phys. Rev. A*, vol. 42, pp. 5675–5683, 1990.

[14] Y. Z. Hu, R. Binder, S. W. Koch, S. T. Cundiff, H. Wang, and D. G. Steel, "Excitation and polarization effects in semiconductor 4-wave-mixing spectroscopy," *Phys. Rev. B*, vol. 49, pp. 14 382–14 386, 1994.

[15] H. Wang, K. B. Ferrio, D. G. Steel, P. R. Berman, Y. Z. Hu, R. Binder, and S. W. Koch, "Transient 4-wave-mixing line-shapes - effects of excitation-induced dephasing," *Phys. Rev. A*, vol. 49, pp. R1551–R1554, 1994.

[16] H. L. Wang, K. Ferrio, D. G. Steel, Y. Z. Hu, R. Binder, and S. W. Koch, "Transient nonlinear-optical response from excitation induced dephasing in gaas," *Phys. Rev. Lett.*, vol. 71, pp. 1261–1264, 1993.

[17] K. Bott, O. Heller, D. Bennhardt, S. T. Cundiff, P. Thomas, E. J. Mayer, G. O. Smith, R. Eccleston, J. Kuhl, and K. Ploog, "Influence of exciton-exciton interactions on the coherent optical-response in gaas quantum-wells," *Phys. Rev. B*, vol. 48, pp. 17 418–17 426, 1993.

[18] J. M. Shacklette and S. T. Cundiff, "Nonperturbative transient four-wave-mixing line shapes due to excitation-induced shift and excitation-induced dephasing," *J. Opt. Soc. Am. B*, vol. 20, pp. 764–769, 2003.

[19] J. M. Shacklette and S. T. Cundiff, "Role of excitation-induced shift in the coherent optical response of semiconductors," *Phys. Rev. B*, vol. 66, p. 045309, 2002.

[20] V. M. Axt and A. Stahl, "A dynamics-controlled truncation scheme for the hierarchy of density-matrices in semiconductor optics," *Z. für Physik B*, vol. 93, pp. 195–204, 1994.

[21] V. M. Axt and A. Stahl, "The role of the biexciton in a dynamic density-matrix theory of the semiconductor band-edge," *Z. Für Physik B*, vol. 93, pp. 205–211, 1994.

[22] M. Lindberg, Y. Z. Hu, R. Binder, and S. W. Koch, "$\chi^{(3)}$ formalism in optically-excited semiconductors and its applications in 4-wave-mixing spectroscopy," *Phys. Rev. B*, vol. 50, pp. 18 060–18 072, 1994.

[23] Y. Tanimura and S. Mukamel, "2-dimensional femtosecond vibrational spectroscopy of liquids," *J. Chem. Phys.*, vol. 99, pp. 9496–9511, 1993.

[24] M. C. Asplund, M. T. Zanni, and R. M. Hochstrasser, "Two-dimensional infrared spectroscopy of peptides by phase-controlled femtosecond vibrational photon echoes," *Proc. Nat. Acad. Sci. USA*, vol. 97, pp. 8219–8224, 2000.

[25] O. Golonzka, M. Khalil, N. Demirdöven, and A. Tokmakoff, "Vibrational anharmonicities revealed by coherent two-dimensional infrared spectroscopy," *Phys. Rev. Lett.*, vol. 86, pp. 2154–2157, 2001.

[26] J. Hybl, A. Ferro, and D. Jonas, "Two-dimensional Fourier transform electronic spectroscopy," *J. Chem. Phys.*, vol. 115, no. 14, pp. 6606–6622, 2001.

[27] T. Brixner, J. Stenger, H. Vaswani, M. Cho, R. Blankenship, and G. Fleming, "Two-dimensional spectroscopy of electronic couplings in photosynthesis," *Nature*, vol. 434, pp. 625–628, 2005.

[28] M. Khalil, N. Demirdoven, and A. Tokmakoff, "Obtaining absorptive line shapes in two-dimensional infrared vibrational correlation spectra," *Phys. Rev. Lett.*, vol. 90, pp. 047401–047404, 2003.

[29] K. Leo, T. C. Damen, J. Shah, E. O. Göbel, and K. Kohler, "Quantum beats of light hole and heavy hole excitons in quantum wells," *Appl. Phys. Lett.*, vol. 57, pp. 19–21, 1990.

[30] E. O. Göbel, K. Leo, T. C. Damen, J. Shah, S. Schmitt-Rink, W. Schäfer, J. F. Muller, and K. Köhler, "Quantum beats of excitons in quantum-wells," *Phys. Rev. Lett.*, vol. 64, pp. 1801–1804, 1990.

[31] M. Koch, J. Feldmann, G. von Plessen, E. O. Göbel, P. Thomas, and K. Kohler, "Quantum beats versus polarization interference—an experimental distinction," *Phys. Rev. Lett.*, vol. 69, pp. 3631–3634, 1992.

[32] V. G. Lyssenko, J. Erland, I. Balslev, K. H. Pantke, B. S. Razbirin, and J. M. Hvam, "Nature of nonlinear 4-wave-mixing beats in semiconductors," *Phys. Rev. B*, vol. 48, pp. 5720–5723, 1993.

[33] F. Jahnke, M. Koch, T. Meier, J. Feldmann, W. Schäfer, H. Nickel, P. Thomas, S. W. Koch, and E. O. Göbel, "Simultaneous influence of disorder and coulomb interaction on photon-echoes in semiconductors," *Phys. Rev. B*, vol. 50, pp. 8114–8117, 1994.

[34] M. Koch, J. Feldmann, E. O. Göbel, P. Thomas, J. Shah, and K. Köhler, "Coupling of exciton-transitions associated with different quantum-well islands," *Phys. Rev. B*, vol. 48, pp. 11 480–11 483, 1993.

[35] A. Euteneuer, E. Finger, M. Hofmann, W. Stolz, T. Meier, P. Thomas, S. W. Koch, W. W. Rühle, R. Hey, and K. Ploog, "Coherent excitation spectroscopy on inhomogeneous exciton ensembles," *Phys. Rev. Lett.*, vol. 83, pp. 2073–2076, 1999.

[36] S. T. Cundiff, M. Koch, W. H. Knox, J. Shah, and W. Stolz, "Optical coherence in semiconductors: Strong emission mediated by nondegenerate interactions," *Phys. Rev. Lett.*, vol. 77, pp. 1107–1110, 1996.

[37] I. Kuznetsova, P. Thomas, T. Meier, T. Zhang, X. Li, R. P. Mirin, and S. T. Cundiff, "Signatures of many-particle correlations in two-dimensional Fourier-transform spectra of semiconductor nanostructures," *Solid State Comm.*, vol. 142, pp. 154–158, 2007.

[38] S. T. Cundiff, T. Zhang, A. D. Bristow, D. Karaiskaj, and X. Dai, "Optical two-dimensional fourier transform spectroscopy of semiconductor quantum wells," *Acc. Chem. Res.*, vol. 42, pp. 1423–1432, 2009.

[39] L. J. Yang, I. V. Schweigert, S. T. Cundiff, and S. Mukamel, "Two-dimensional optical spectroscopy of excitons in semiconductor quantum wells: Liouville-space pathway analysis," *Phys. Rev. B*, vol. 75, p. 125302, 2007.

[40] L. Yang, T. Zhang, A. D. Bristow, S. T. Cundiff, and S. Mukamel, "Isolating excitonic raman coherence in semiconductors using two-dimensional correlation spectroscopy," *J. Chem. Phys.*, vol. 129, p. 234711, 2008.

[41] K. W. Stone, D. B. Turner, K. Gundogdu, S. T. Cundiff, and K. A. Nelson, "Exciton-exciton correlations revealed by two-quantum two-dimensional fourier transform optical spectroscopy," *Acct. Chem. Res.*, vol. 42, pp. 1452–1461, 2009.

[42] I. Kuznetsova, T. Meier, S. T. Cundiff, and P. Thomas, "Determination of homogeneous and inhomogeneous broadening in semiconductor nanostructures by two-dimensional fourier-transform optical spectroscopy," *Phys. Rev. B*, vol. 76, p. 153301, 2007.

[43] M. E. Siemens, G. Moody, H. Li, A. D. Bristow, and S. T. Cundiff, "Resonance lineshapes in two-dimensional fourier transform spectroscopy," *Opt. Express*, vol. 18, no. 17, pp. 17 699–17 708, 2010.

[44] A. D. Bristow, T. Zhang, M. E. Siemens, S. T. Cundiff, and R. P. Mirin, "Separating homogeneous and inhomogeneous line widths of heavy- and light-hole excitons in weakly disordered semiconductor quantum wells," *J. Phys. Chem. B*, http://dx.doi.org/10.1021/jp109408s, 2011.

[45] G. Moody, M. E. Siemens, A. D. Bristow, X. Dai, D. Karaiskaj, A. S. Bracker, D. Gammon, and S. T. Cundiff, "Exciton-exciton and exciton-phonon interactions in an interfacial gaas quantum dot ensemble," *Phys. Rev. B*, vol. 83, 115324, 2011.

[46] W. Langbein and B. Patton, "Heterodyne spectral interferometry for multidimensional nonlinear spectroscopy of individual quantum systems," *Opt. Lett.*, vol. 31, pp. 1151–1153, 2006.

[47] J. Kasprzak, B. Patton, V. Savona, and W. Langbein, "Coherent coupling between distant excitons revealed by two-dimensional nonlinear hyperspectral imaging," *Nat. Photon.*, vol. 5, no. 1, pp. 57–63, Jan. 2011.

[48] A. D. Bristow, D. Karaiskaj, X. Dai, T. Zhang, C. Carlsson, K. R. Hagen, R. Jimenez, and S. T. Cundiff, "A versatile ultrastable platform for optical multidimensional Fourier-transform spectroscopy," *Rev. Sci. Instr.*, vol. 80, no. 7, pp. 0731081–0731088, Jul. 2009.

[49] L. Lepetit, G. Cheriaux, and M. Joffre, "Linear techniques of phase measurement by femtosecond spectral interferometry for applications in spectroscopy," *J. Opt. Soc. Am. B*, vol. 12, p. 2467, 1995.

[50] A. D. Bristow, D. Karaiskaj, X. Dai, and S. T. Cundiff, "All-optical retrieval of the global phase for twodimensional fourier-transform spectroscopy," *Opt. Express*, vol. 16, pp. 18 017–18 027, 2008.

[51] E. H. G. Backus, S. Garrett-Roe, and P. Hamm, "Phasing problem of heterodyne-detected two-dimensional infrared spectroscopy," *Opt. Lett.*, vol. 33, pp. 2665–2667, 2008.

[52] I. Kuznetsova, N. Gogh, J. Foerstner, T. Meier, S. T. Cundiff, I. Varga, and P. Thomas, "Modeling excitonic line shapes in weakly disordered semiconductor nanostructures," *Phys. Rev. B*, vol. 81, no. 7, pp. 075307–075316, Feb. 2010.

[53] S. Faeder and D. Jonas, "Two-dimensional electronic correlation and relaxation spectra: Theory and model calculations," *J. Phys. Chem. A*, vol. 103, no. 49, pp. 10 489–10 505, 1999.

[54] A. Tokmakoff, "Two-dimensional line shapes derived from coherent third-order nonlinear spectroscopy," *J. Phys. Chem. A*, vol. 104, no. 18, pp. 4247–4255, May 11, 2000.

[55] I. Kuznetsova, P. Thomas, T. Meier, T. Zhang, and S. T. Cundiff, "Determination of homogeneous and inhomogeneous broadenings of quantum-well excitons by 2DFTS: An experiment-theory comparison," *Physica Status Solidi (c)*, vol. 6, no. 2, pp. 445–448, Feb. 2009.

[56] A. Honold, L. Schultheis, J. Kuhl, and C. W. Tu, "Collision broadening of two-dimensional excitons in a gaas single quantum well," *Phys. Rev. B*, vol. 40, no. 9, pp. 6442–6445, 1989.

[57] S. D. Baranovskii and A. L. Efros, "Band edge smearing in solid-solutions," *Soviet Phys. Semicon.*, vol. 12, no. 11, pp. 1328–1330, 1978.

[58] L. Schultheis, J. Kuhl, A. Honold, and C. W. Tu, "Ultrafast phase relaxation of excitons via exciton-exciton and exciton-electron collisions," *Phys. Rev. Lett.*, vol. 57, pp. 1635–1638, 1986.

[59] A. Zrenner, L. V. Butov, M. Hagn, G. Abstreiter, G. Böhm, and G. Weimann, "Quantum dots formed by interface fluctuations in alas/gaas coupled quantum well structures," *Phys. Rev. Lett.*, vol. 72, no. 21, pp. 3382–3385, May 1994.

[60] K. Brunner, G. Abstreiter, G. Böhm, G. Trönkle, and G. Weimann, "Sharp-line photoluminescence and 2-photon absorption of zero-dimensional biexcitons in a gaas/algaas structure," *Phys. Rev. Lett.*, vol. 73, no. 8, pp. 1138–1141, 1994.

[61] H. Hess, E. Betzig, T. Harris, L. Pfeiffer, and K. West, "Near-field Spectroscopy Of The Quantum Constituents Of A Luminescent System," *Science*, vol. 264, no. 5166, pp. 1740–1745, Jun. 17, 1994.

[62] D. Gammon, E. Snow, and D. Katzer, "Excited-state spectroscopy of excitons in single quantum dots," *Appl. Phys. Lett.*, vol. 67, no. 16, pp. 2391–2393, Oct. 1995.

[63] D. Gammon, E. Snow, B. Shanabrook, D. Katzer, and D. Park, "Homogeneous linewidths in the optical spectrum of a single gallium arsenide quantum dot," *Science*, vol. 273, pp. 87–90, Jul. 1996.

[64] J. Guest, T. Stievater, X. Li, J. Cheng, D. Steel, D. Gammon, D. Katzer, D. Park, C. Ell, A. Thranhardt, G. Khitrova, and H. Gibbs, "Measurement of optical absorption by a single quantum dot exciton," *Phys. Rev. B*, vol. 65, no. 24, pp. 1310–1313, Jun. 2002.

[65] N. Bonadeo, J. Erland, D. Gammon, D. Park, D. Katzer, and D. Steel, "Coherent optical control of the quantum state of a single quantum dot," *Science*, vol. 282, no. 5393, pp. 1473–1476, Nov. 20, 1998.

[66] E. Muljarov and R. Zimmermann, "Dephasing in quantum dots: Quadratic coupling to acoustic phonons," *Phys. Rev. Lett.*, vol. 93, no. 23, pp. 7401–7404, Dec. 2004.

[67] T. Takagahara, "Theory of exciton dephasing in semiconductor quantum dots," *Phys. Rev. B*, vol. 60, no. 4, pp. 2638–2652, Jul. 15, 1999.

[68] X. Fan, T. Takagahara, J. Cunningham, and H. Wang, "Pure dephasing induced by exciton-phonon interactions in narrow GaAs quantum wells," *Sol. State Commun.*, vol. 108, no. 11, pp. 857–861, Nov. 1998.

[69] E. Peter, J. Hours, P. Senellart, A. Vasanelli, A. Cavanna, J. Bloch, and J. Gerard, "Phonon sidebands in exciton and biexciton emission from single GaAs quantum dots," *Phys. Rev. B*, vol. 69, no. 4, pp. 1307–1310, Jan. 2004.

[70] P. Borri, W. Langbein, S. Schneider, U. Woggon, R. L. Sellin, D. Ouyang, and D. Bimberg, "Ultralong dephasing time in ingaas quantum dots," *Phys. Rev. Lett.*, vol. 87, no. 15, pp. 7401–7404, 2001.

[71] D. Gammon, E. Snow, B. Shanabrook, D. Katzer, and D. Park, "Fine structure splitting in the optical spectra of single GaAs quantum dots," *Phys. Rev. Lett.*, vol. 76, no. 16, pp. 3005–3008, Apr. 1996.

Steven T. Cundiff (M'98–SM'11) received the B.A. degree in physics from Rutgers University, New Brunswick, NJ, in 1985, and the M.S. and Ph.D. degrees in applied physics from the University of Michigan, Ann Arbor, in 1991 and 1992, respectively.

He spent two years as an Alexander von Humboldt Fellow at the University of Marburg, Germany, and then joined Bell Laboratories, Holmdel, NJ, as a Postdoctoral Member of Technical Staff. In 1997, he joined JILA, a joint institute between the University of Colorado and the National Institute of Standards and Technology (NIST), in Boulder, Colorado. He is a Fellow of the Joint Institute for Laboratory Astrophysics (JILA), a Physicist with the NIST Quantum Physics Division, and a Professor Adjoint at the University of Colorado Department of Physics and Electrical and Computer Engineering Department.

Prof. Cundiff is a Fellow of the Optical Society of America and of the American Physical Society.

Alan D. Bristow received the B.Sc. degree in interdisciplinary physics from the University of East Anglia, Norwich, U.K., in 1997, and the M.Sc. degree in optoelectronics and laser devices from Heriot-Watt University, Edinburgh, Scotland, U.K., in 1998, and the Ph.D. degree in physics from the University of Sheffield, Sheffield, South Yorkshire, U.K., in 2003.

He was a Postdoctoral Fellow at the University of Toronto in Canada for three years, and then a Research Associate at Joint Institute for Laboratory Astrophysics (JILA, a joint institute between the National Institute of Standards and Technology and the University of Colorado) for an additional three years. In 2009, he was an Adjunct Instructor at Colorado School of Mines. Since 2010, he has been an Assistant Professor in the Department of Physics at West Virginia University, Morgantown.

Prof. Bristow is a member of the American Physical Society, the Optical Society of America, and the West Virginia WVNano Initiative.

Mark Siemens received the B.S. degree in engineering physics from the Colorado School of Mines, in 2003, and the Ph.D. degree in physics from the Joint Institute for Laboratory Astrophysics (JILA, a joint institute between the National Institute of Standards and Technology and the University of Colorado) and the University of Colorado, in 2009.

After graduating in 2009, he worked as an NRC Postdoc at the National Institute of Standards and Technology (NIST) and JILA. In 2010, he moved to the University of Denver, where he joined the Department of Physics and Astronomy as an Assistant Professor.

Hebin Li received the Ph.D. degree in physics from Texas A&M University, in 2010.

He is currently a Postdoctoral Research Associate at the Joint Institute for Laboratory Astrophysics (JILA, a joint institute between the University of Colorado and the National Institute of Standards and Technology (NIST), in Boulder, Colorado.

Galan Moody received the B.S. degree in engineering physics from the University of Colorado at Boulder, in 2008, and is currently a graduate student in Dr. Cundiff's group.

His research interests are in light-matter interactions in condensed-matter nanostructures.

Denis Karaiskaj received the Diploma in physics from the Philipps University of Marburg, Germany, and the Ph.D. degree in physics from Simon Fraser University, British Columbia, Canada.

He was a Postdoctoral Scientist at the University of California, Irvine, Postdoctoral Fellow and Research Associate at the National Renewable Energy Laboratory (NREL) in Golden, Colorado, and at the Joint Institute for Laboratory Astrophysics (JILA) (CU & NIST) in Boulder, Colorado. Currently, he is a Faculty at the University of South Florida in Tampa, Florida.

Xingcan Dai received the B.S. and M.S. degrees in physics from Tsinghua University of China, in 1997 and 2000, respectively, and the Ph.D. degree in physics, in 2006, from the University of California, Berkeley.

He was a Research Associate at the Joint Institute for Laboratory Astrophysics (JILA) between 2007 and 2010. Since March 2010, he is working at the Department of Physics at Tsinghua University of China, Beijing, China, as an Assistant Professor.

Tianhao Zhang received the B.S. degree in physics in 1997, from the University of Science and Technology of China, Hefei, Anhui, China, and the M.S. and Ph.D. degrees in physics from the Joint Institute for Laboratory Astrophysics (JILA), National Institute of Standards and Technology (NIST) and University of Colorado at Boulder, in 2002 and 2008, respectively.

He is currently a Postdoctoral Research Associate at the College of Nanoscale Science and Engineering, State University of New York at Albany.